

# SNAP: A Software Package for User-Guided Geodesic Snake Segmentation

Sean Ho <sup>\*</sup>, Heather Cody <sup>\*\*</sup>, Guido Gerig

Department of Computer Science

<sup>\*</sup> <sup>\*\*</sup> Department of Psychiatry

University of North Carolina, Chapel Hill, NC 27599, USA

seanho@cs.unc.edu

**Abstract.** We present a new software package for interactive segmentation of 3D images by geodesic snakes, with manual editing. Several variants of level set snakes are incorporated, including both gradient-magnitude based snakes as well as region-competition snakes. A complete segmentation pipeline, including image preprocessing, bubble initialization and parameter control, is provided in an intuitive user interface. Slice-based overpainting is also provided in the same framework, for manual editing of the automatic snake segmentation. This tool is already in daily use by clinicians and offers a vast improvement in speed over traditional manual segmentation. We present examples from several clinical studies, as well as validation results comparing the automatic geodesic snakes segmentation with manual expert rater segmentation.

## 1 Introduction

Segmentation of volumetric image data is still a challenging problem, and while there is much exciting research on new methods for fully automatic segmentation, clinical users have an immediate need for well-developed, easy-to-use software tools to aid the user in segmentation. As research progresses on new methodology, there should be a parallel “trickle-down” of technology in the form of software systems such that clinical users with minimal computer science background can make use of the new methods. In many places, the state-of-the-art in segmentation is still manual slice-by-slice outlining, requiring several hours to segment objects for example within the brain. Methods that are relatively well-known in the research community can dramatically ease the segmentation task, but many of these methods are currently implemented only in research testbeds, not available to the user community. In order to be used more widely, the methods must be encapsulated in an easy-to-use interface which keeps the user in the loop. The SNAP software package is now in daily use by clinicians, and provides a comprehensive geodesic snake segmentation toolset for users.

The automatic segmentation tools SNAP provides to assist the user implement the well-known geodesic snakes, also known as level set snakes or implicit

---

<sup>\*</sup> Supported by NIH-NCI P01 CA47982.

<sup>\*\*</sup> Supported by NIH RO1 MH61696 (PI: Joe Piven)

snakes. Geodesic snakes are appealing especially for volumetric data processing due to their elegant formulation as nonlinear PDE's [1–4] [5, 6]. The formalism can be naturally extended from 2-D to higher dimensions, and the resulting zero level sets offer flexible topology. The geodesic snakes in SNAP implement several varieties of snakes presented in the literature, both boundary-driven and region-based snakes. Therefore, users can select the most appropriate method and optimally tune parameters for specific tasks. These are discussed in Section 2. SNAP has already been applied to a wide variety of segmentation projects, including gray-matter subcortical structures, abdominal CT, and brain tumors in MRI; these are shown in Section 3. In Section 4, validation results are shown comparing SNAP's geodesic snake segmentation to manual segmentation of the caudate nucleus in brain MRI. The validation results demonstrate that while there are (well-understood) limitations to automatic geodesic snake segmentation, SNAP's integration of automatic methods with user editing greatly helps the user in manual segmentation.

## 2 Geodesic Snakes

Level set evolution with fixed propagation direction as in boundary-driven snakes [2, 4] is initialized either inside or outside of sought objects, and the propagation force is locally opposed by a strong gradient magnitude at image discontinuities to stop propagation. Global smoothness guarantees stability in the presence of small gaps in boundaries. An alternate concept of level set evolution is region competition, where object and background regions compete for their common boundary [7], additionally constrained by a smoothness term. It is important to notice that in region-based snakes, a crucial part of the segmentation problem is shifted to the preprocessing step that provides region interior/exterior probabilities. The following subsections present a common formalism for both types of implicit snakes, as implemented in SNAP.

### 2.1 Boundary-driven snakes

**Implicit geodesic snakes** Following the mathematical notion of [4], the level set snake  $\mathbf{C}(u) = (C_x, C_y)$  is defined as the zero level set of an implicit function  $\varphi$  defined on the entire image. The evolution of the snake is defined via a partial differential equation on the implicit function  $\varphi$ . We use the following formula:

$$\begin{aligned} \frac{\partial \varphi}{\partial t} = & c_{\text{MCF}} \cdot (g)^{r_{\text{MCF}}+1} \text{div} \left( \frac{\nabla \varphi}{|\nabla \varphi|} \right) |\nabla \varphi| + \\ & (g)^{r_{\nabla g}} (\nabla g) \cdot \nabla \varphi + (g)^{r_c} \alpha |\nabla \varphi| + c_s \cdot (g)^{r_s} \nabla^2 \varphi, \end{aligned}$$

We have four terms in the formula. The first is the MCF (Mean Curvature Flow) term, which smoothes out the curve in the absence of a boundary. The second is the  $\nabla g$  term, which attracts the curve into the boundary. The third

is the  $\alpha$  term, which is a constant velocity. Finally, we have a  $\nabla^2\varphi$  term to smooth  $\varphi$  over time in order to avoid numerical instability. Each of these four terms are modulated by  $g = g(|\nabla I|)$ , a monotonic function of the image gradient magnitude, to slow down curve evolution at the boundary.

We introduce four nonnegative integer constants  $r_{\text{MCF}}$ ,  $r_{\nabla g}$ ,  $r_c$ , and  $r_s$ , and two real coefficients  $c_{\text{MCF}}$  and  $c_s$ , to modulate each of the four terms. This formula can serve as a unified framework to describe and compare different types of gradient-magnitude based geodesic snakes.

## Various formulations of implicit snakes

1. Goldenberg's version [4]

**coeff:**  $c_{\text{MCF}}: 1$   $r_{\text{MCF}}: 1$   $r_{\nabla g}: 1$   $r_c: 1$   $c_s: 0$   $r_s: -$

$$\frac{\partial\varphi}{\partial t} = g(I) \left( \alpha + \text{div} \left( g(I) \frac{\nabla\varphi}{|\nabla\varphi|} \right) \right) |\nabla\varphi| = g(I) (\alpha + \text{div}(g(I)\nabla\varphi)) \quad (|\nabla\varphi| = 1)$$

2. Caselles' version [2]

**coeff:**  $c_{\text{MCF}}: 1$   $r_{\text{MCF}}: 0$   $r_{\nabla g}: 0$   $r_c: 1$   $c_s: 0$   $r_s: -$

$$\frac{\partial\varphi}{\partial t} = |\nabla\varphi| \text{div} \left( g(I) \frac{\nabla\varphi}{|\nabla\varphi|} \right) + \alpha g(I) |\nabla\varphi| .$$

3. 'Own version' using additional stability term on  $\varphi$

**coeff:**  $c_{\text{MCF}}: 1$   $r_{\text{MCF}}: 1$   $r_{\nabla g}: 1$   $r_c: 2$   $c_s: 1$   $r_s: 2$

$$\frac{\partial\varphi}{\partial t} = g(I) \left[ |\nabla\varphi| \text{div} \left( g(I) \frac{\nabla\varphi}{|\nabla\varphi|} \right) + \alpha g(I) |\nabla\varphi| + g(I) \nabla^2\varphi \right]$$

## 2.2 Region-competition snakes

Alternatively to boundary-limited snakes governed by the term  $g(I)$ , a snake can be controlled by local probabilities to be inside or outside of sought structures. In region-based snakes, the constant propagation term  $\alpha$  is modulated by a image force term to locally change direction and speed of propagation, so that the snake shrinks when the boundary encloses parts of the background (B), and grows when the boundary is inside the wanted regions (A). This framework provides a competition between objects and background [7] and thus reaches an equilibrium stage at convergence. A common choice is the term  $\alpha(P(A(x)) - P(B(x)))$ , where  $P(A(x))$  and  $P(B(x))$  are obtained by statistical classification or histogram analysis. In SNAP, an interface is provided to derive  $P(A)$  and  $P(B)$  from thresholds on the image; a pre-made map of  $P(A) - P(B)$  can also be loaded from disk. As in the previous discussion, the image forces need to be balanced with smoothness constraints (MCF), and the FTCS (forward in time

centered space) discrete solution of the PDE can be additionally stabilized by a uniform smoothing of the implicit function  $\varphi$ , resulting in:

$$\frac{\partial \varphi}{\partial t} = c_{\text{MCF}} |\nabla \varphi| \operatorname{div} \left( \frac{\nabla \varphi}{|\nabla \varphi|} \right) + \alpha (P(A) - P(B)) |\nabla \varphi| + c_s \nabla^2 \varphi.$$

### 3 Applications

We present several applications of SNAP, serving as examples for the large spectrum of 3-D object segmentation tasks processed in our medical image analysis lab using SNAP. Later, in Section 4, we will discuss one application in particular, the caudate nucleus, including validation of the automatic segmentation against manual raters.

#### 3.1 Hippocampus segmentation

Deep gray-matter structures such as the hippocampus and caudate nucleus are both known to present challenging segmentation problems in MRI. Currently, these are most often solved by a tedious slice-by-slice boundary drawing with limited reliability. Gradient-magnitude based snakes can greatly speed the reliable segmentation of these structures; the snakes work particularly well in high-resolution (e.g. 1x1x1mm) T1 MRIs such as those afforded by new 3T scanners. Snakes do not work perfectly, though, for these complex structures; for example, the hippocampal-amygdala transition area (HATA) does not always provide a strong enough boundary to stop the snake. The user interface in SNAP allows the user easily to stop the snake at an appropriate place, and manually edit the segmentation if needed. The segmentations shown in Figures 1 and 2 were done in just a few minutes.

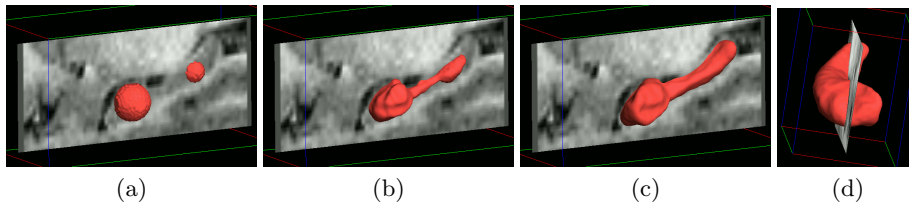


**Fig. 1.** Segmentation of left hippocampus from MRI: (a) initialization by two bubbles, (b) 6 iterations, (c) 18 iterations (final), and (d) final segmentation with rotated view ( $c_{\text{MCF}} = 1$ ,  $r_{\text{MCF}} = -1$ ,  $r_{\nabla g} = 1$ ,  $r_c = 2$ ,  $\alpha = 1.4$ ,  $r_s = 0$ , and  $c_s = 0.8$ ).

#### 3.2 Brain tumor segmentation

Accurate and efficient segmentation of 3-D tumor structures is routinely required in radiotherapy planning and in surgical planning. Tumor segmentation is challenging because of the variable appearance (size, location, boundary complexity,

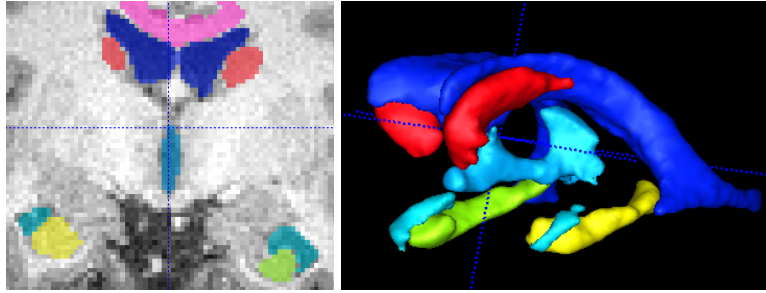


**Fig. 2.** Gradient-magnitude based snake segmentation of several subcortical structures from high-resolution T1-weighted MRI, including hippocampus, amygdala, caudate, and ventricles

contrast, interior texture, surrounding edema) of various tumor types. SNAP has successfully been used to segment several complex meningiomas and glioblastomas in contrast-enhanced MRIs (Figure 3), with excellent validation results when compared to human rater manual segmentation [8].

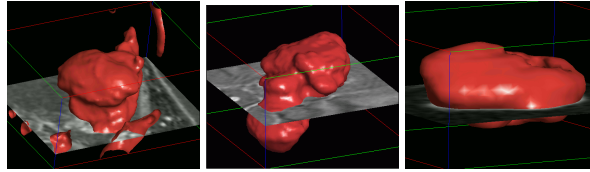


**Fig. 3.** Region-based snake segmentations (300 iterations) of three tumor datasets Tumor022, Tumor025, and Tumor026. A preliminary machine versus human rater validation [8] showed over 90% overlap and less than 1mm average boundary distance.

### 3.3 Liver segmentation from CT

SNAP allows the user easy access to change parameters to adapt the snakes to different imaging modalities. The high contrast in CT provides for easy segmentation; it took less than 10 minutes to find appropriate parameters to segment the liver and ribs shown in Figure 4.

## 4 Validation: Caudate Study

The caudate nucleus is a structure of interest in many studies of mental illness and neurological diseases. There is a clinical hypothesis that the caudate is associated with the ritualistic, repetitive behaviors seen in autism. Due to limited voxel resolution of today's routine MRI scans (roughly  $1 \times 1 \times 1.5 \text{mm}^3$ ) and complex contrast variability along the boundary, reliable segmentation is considered an extremely difficult task. The manual segmentation is very time

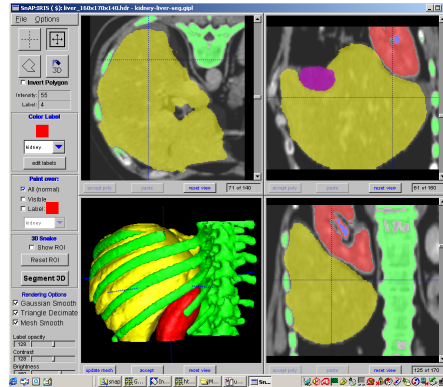


**Fig. 4.** Segmentation of the liver and ribs from abdominal CT, done in SNAP in less than 10 minutes.

consuming as it takes 3–4 hours for trained experts to reliably segment the left and right structures. As an alternative, we test the performance of geodesic snakes in comparison to human rater gold standards. We preprocess the images by performing a standard statistical pattern recognition fuzzy classification of the multi-channel MRIs into gray-matter, white-matter, and CSF (cerebro-spinal fluid) tissue classes. Since the caudate is a gray-matter structure, the user then loads the fuzzy gray-matter classification map into SNAP. The snake process is initialized as a set of bubbles in the caudate. Alternatively, we could also use a coarse region of interest placed inside the structure. The evolution propagates outwards and, given a balance between propagation and opposing boundary forces, converges in the head and main body of the caudate. The tail of the caudate shares an ill-defined boundary with an adjacent gyrus, so the snake, if left to run on its own, would bleed into nearby structures. Our tool allows the user to stop propagation and to edit the result of the snake segmentation, mostly by providing a few cutting lines to define the end of the caudate tail. The whole process including manual corrections takes about 5-10 minutes, which has to be compared with the 3–4 hours of purely manual region definition.

To validate the snake segmentation in SNAP against manual segmentation, MRIs from 5 patients were used, replicated 3 times each (segmenter was blinded to replications), and both left and right caudates were segmented by both a user with SNAP as well as a single manual rater. In total we had  $5 \times 3 \times 2 = 60$  caudate segmentations. We then looked at the segmented volumes to compare the results. SNAP-assisted and all-manual segmentation both showed very high intra-rater reliability, as shown in Figure 5.

|                             |       |
|-----------------------------|-------|
| All-manual segmentation:    | 98.4% |
| SNAP-assisted segmentation: | 99.2% |

**Fig. 5.** Intra-rater reliability on segmented caudate volumes. 5 patients were each segmented 3 times, both left and right caudates.

Comparing the segmented caudate volumes from the SNAP-assisted segmentation to the “ground-truth” of the manual rater, the geodesic snakes seemed to segment slightly larger caudates than the manual rater, as shown in Figure 6. The differences average about 6.1% of the total caudate volume. The preprocessing step has a strong influence on the boundary to which the snake converges; a slight change in the fuzzy gray-matter classification significantly changes the volume of the snake-segmented caudate. In addition, the tail of the caudate blends seamlessly into a neighboring gyrus, so the manual rater must decide where to stop, and the SNAP user must interactively halt the progression of the snake. As seen in Figure 7, the SNAP-assisted and fully manual segmentations agree quite well overall.



**Fig. 6.** Comparison of segmented caudate volumes (in  $mm^3$ ) for all 30 instances (5 patients, 3 repetitions, left/right). Volumes from manual segmentation are on left; volumes using SNAP are on right.

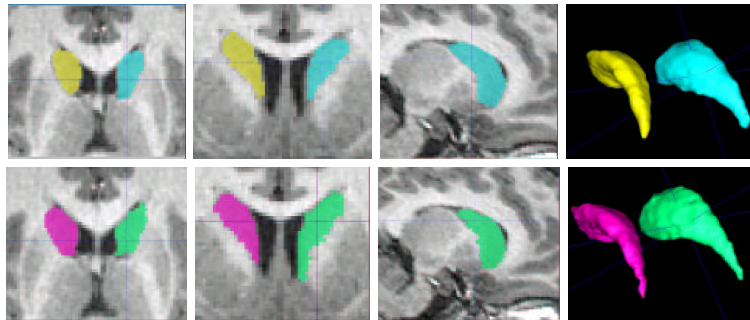


**Fig. 7.** Comparison of caudate segmentation (both left and right caudates) by user with SNAP (top row) and by manual rater (bottom row).

## 5 Conclusions

We demonstrate a common framework for 3-D level set evolution. The SNAP software simulates various types of implicit snakes. A user can choose the most

appropriate type of snake and can optimally tune the parameters for various segmentation tasks. The choice between boundary-driven snakes and region-based snakes also requires different types of preprocessing, which are included as part of the software tool. In boundary-driven snakes, the most important parameters are the choice of an appropriate  $g(I)$  function, the degree of smoothness, and finally the propagation speed. In region-based snakes, a user can train statistics about interior and exterior regions by choosing test regions. SNAP is already in use in many clinical applications, and is freely available from <http://midag.cs.unc.edu/>. A new version is presently under development which will integrate with the ITK framework.

## 6 Acknowledgments

SNAP is a fork of the IRIS software project, and was developed primarily by a sequence of three student software development teams at the Department of Computer Science at the University of North Carolina at Chapel Hill, under the supervision of Guido Gerig. The gradient-magnitude geodesic snake code was based on an earlier project supervised by Gabor Székely at ETH Zürich.

## References

1. H. Tek and B.B. Kimia, “Image segmentation by reaction-diffusion bubbles,” in *International Conference on Computer Vision (ICCV)*, 1995, pp. 156–162.
2. V. Caselles, R. Kimmel, and G. Sapiro, “Geodesic active contours,” *International Journal of Computer Vision*, 1997.
3. H. Tek and B.B. Kimia, “Volumetric segmentation of medical images by three-dimensional bubbles,” *Computer Vision and Image Understanding (CVIU)*, vol. 65, no. 2, pp. 246–258, 1997.
4. R. Goldenberg, R. Kimmel, E. Rivlin, and M. Rudzsky, “Fast geodesic active contours,” in *Scale-Space Theories in Computer Vision*, 1999, pp. 34–45.
5. Gozde Unal, Hamid Krim, and Anthony Yezzi, “Stochastic differential equations and geometric flows,” *IEEE Transactions on Image Processing*, vol. 11, no. 12, pp. 1405–1416, Dec 2002.
6. Roman Goldenberg, Ron Kimmel, Ehud Rivlin, and Michael Rudzsky, “Cortex segmentation: A fast variational geometric approach,” *IEEE Transactions on Medical Imaging (TMI)*, vol. 21, no. 12, pp. 1544–1551, Dec 2002.
7. S. Zhu and A. Yuille, “Region competition: Unifying snakes, region growing, and Bayes/MDL for multi-band image segmentation,” in *International Conference on Computer Vision (ICCV)*, 1995, pp. 416–423.
8. Sean Ho, Elizabeth Bullitt, and Guido Gerig, “Level-set evolution with region competition: Automatic 3-d segmentation of brain tumors,” in *International Conference on Pattern Recognition (ICPR’02)*, 2002.